J. Indian Inst. Sci., Sep.–Oct. 2005, **85**, 295–305
© Indian Institute of Science.

Performance evaluation of solar absorption cooling system of Bahal (Haryana)

V. MITTAL[1*], K. S. KASANA[2] AND N. S. THAKUR[3]
[1]Department of Mechanical Engineering, BRCM College of Engg. & Tech., Bahal (Haryana) and
National Institute of Technology (NIT), Kurukshetra, Haryana, India.
email: vmittal1231@rediffmail.com. Phone: 01255-265513 (R); Fax: 01255-265217.
[2]Department of Mechanical Engineering, National Institute of Technology (NIT), Kurukshetra, Haryana, India.
email: kasanaks_nitkkr@rediffmail.com
[3]Department of Mechanical Engineering, National Institute of Technology (NIT), Hamirpur, HP, India.
email: nsthakur@recham.ernet.in.

Received on July 29, 2005; Revised on September 12, 2005.

Abstract

This study presents the modeling of a solar-powered, single-stage, absorption cooling system using a flat plate collector and water–lithium bromide solution. A modular computer program has been developed for the absorption system to simulate various cycle configurations with the help of weather data of village Bahal, Distt. Bhiwani, Haryana, India. The effects of hot water inlet temperatures on the coefficient of performance and the surface area of the absorption cooling component are studied. Also studied is the effect of reference temperature, which is the minimum allowable hot water inlet temperature on the fraction of total load met by nonpurchased energy and coefficient of performance.

Keywords: Solar absorption, flat plate collector, water–lithium bromide solution, cooling, simulation.

1. Introduction

The demand for energy for refrigeration and airconditioning to control temperature and humidity and for fresh air has increased continuously throughout the last decades, especially in developing countries like India. This increase is caused amongst other reasons, by increased thermal loads, occupant comfort demands, and architectural trends. This has been responsible for the escalation of electricity demand and especially for the high peak loads due to the use of electrically driven vapor compression machines. Moreover, the consumption of primary energy and the emission of greenhouse gases associated with electricity generation from fossil fuels lead to considerable environmental consequences and monitory costs. Conventional energy will not be enough to meet the continuously increasing need for energy in the future. In this case, renewable energy sources will become important. An alternative solution for this problem is solar energy, which is available plentiful in most areas, which also represents a good source of thermal energy. Of the various solar airconditioning alternatives, the absorption system appears to be one of the most promising methods [1]. The absorption cycle is similar in certain respects to the electrically driven va-

*Author for correspondence.

por compression machines. Of the various solar absorption airconditioning systems, LiBr-H_2O and H_2O–NH_3 are the major working pairs available. It is reported that LiBr-H_2O pair has higher COP than any other pair of the working fluids. The LiBr-H_2O system operates at a generator temperature in the range of 70–95°C with water used as a coolant in the absorber and condenser [2]. The COP of the system is between 0.6 and 0.8. The major components in the LiBr-H_2O solar absorption cooling systems are chillers and solar collectors. Many researchers have developed solar-assisted absorption refrigeration systems. Most of them have been produced as experimental units. Computer codes have also been written to simulate the systems. Some of these designs are presented here.

Hammad and Audi [3] describes the performance of a nonstorage, continuous, solar-operated absorption refrigeration cycle. The maximum ideal coefficient of performance of the system was determined to be equal to 1.6, while the peak actual coefficient of performance was determined to be equal to 0.55.

Haim *et al.* [4] performed a simulation and analysis of two open-cycle absorption systems. Both systems comprise a closed absorber and evaporator as in conventional single-stage chillers. The regenerator, used to reconcentrate the absorber solution by means of solar energy, makes up the open part of the cycle. The analysis was performed with a computer code developed for modular simulation of absorption systems under varying cycle configurations (open- and closed-cycle systems) and with different working fluids. Based on the specified design features, the code calculates the operating parameters in each system. Results indicate a definite performance advantage for the direct-regeneration system over the indirect one.

Hawlader *et al.* [5] developed a lithium bromide absorption cooling system employing an 11*11 m collector/regenerator unit. They have also developed a computer model, which they validated against real experimental values with good agreement. The experimental results showed a regeneration efficiency varying between 38 and 67% and the corresponding cooling capacities ranged from 31 to 72 kW.

Ameel *et al.* [6] gives performance predictions of alternative low-cost absorbents for open cycle absorption using a number of absorbents. The most promising of the absorbents considered was a mixture of two elements, lithium chloride and zinc chloride. The estimated capacities per unit absorber area were 50–70% lesser than those of lithium bromide systems.

Li and Sumathy [7] have presented the simulation of a solar-powered absorption airconditioning system with the absorption pair of lithium bromide and water. An attempt was made to increase the COP of the system by partitioning a single storage tank into two parts. Different models of the water storage tank have been presented and analyzed to give a detailed comparison of collector and cooling efficiencies. The system simulation showed that the partitioned hot-water storage tank results in earlier cooling effect, and hence, the overall system COP is higher, compared to a normal stratified storage system.

Florides *et al.* [8] have done the modeling and simulation of an absorption solar-cooling system with the help of TRNSYS simulation program and the typical meteorological year file containing the weather parameters of Nicosia, Cyprus. System optimization was carried out to select the appropriate type of collector, the optimum size of storage tank, the opti-

mum collector slope and area, and the optimum thermostats setting of the auxiliary boiler. The final optimized system consists of a 15 m^2 compound parabolic collector tilted 30° from the horizontal and a 600-l hot water storage tank.

Ghaddar *et al.* [9] studied solar energy utilization in space cooling of a small residential application using a solar lithium bromide absorption system. A simulation program for modeling and performance evaluation of the solar-operated absorption cycle was done for all possible climatic conditions of Beirut. The results have shown that for each ton of refrigeration a minimum collector area of 23.3 m^2 is required with an optimal water storage tank capacity ranging from 1000 to 1500 l for the system to operate solely on solar energy for about seven hours a day.

Assilzadeha *et al.* [10] presented a solar-cooling system that has been designed for Malaysia and similar tropical regions using evacuated tube solar collectors and LiBr absorption unit. The modeling and simulation of the absorption solar-cooling system was carried out with TRNSYS program. The typical meteorological year file containing the weather parameters for Malaysia was used to simulate the system.

Tsilingiris [11] developed a theoretical microcomputer model suitable for performance prediction and investigation of the operational behaviour of a simple cooling system for small residential applications.

Li and Sumathy [12] reported the performance of a modified solar-powered airconditioning system, which is integrated with a partitioned storage tank. In addition, the effect of two main parameters that influence the system performance was presented and discussed. The study showed that by partitioning the storage tank, the solar-cooling effect can be realized much earlier and could attain a total solar-cooling COP of 12% higher compared to the conventional whole-tank mode. Simulation results also indicate that there exists an optimum ratio of storage tank volume over collector area.

Liu and Wang [13] presented the performance prediction of a solar/gas-driving double-effect LiBr–H_2O absorption system. In order to use auxiliary energy more effectively and be less dependent on solar irradiation, a new kind of solar/gas-driving double-effect LiBr–H_2O absorption system was designed.

1.1. *Location of research work*

Bahal is a small town in district Bhiwani on the western fringe of Haryana, bordering Rajasthan. Its latitude and longitude are 29°05′N and 76°28′ E, respectively. The solar insolation on hourly basis for each month of the cooling season, i.e. May to September is measured with the help of pyranometer (solarimeter) and then monthly averages of these values are evaluated. Table I shows the monthly mean values of solar insolation data.

1.2. *Motivation and objective of the present research*

To improve the system design of a solar-powered absorption airconditioning system, a parametric study needs to be carried out to investigate the influence of key parameters on the overall system performance. If experiments were used to perform the parametric study, ef-

Table I
Solar insolation, I (W/m^2), for Bahal, India

Time	Solar insolation (W/m^2)				
	May	June	July	August	September
7:00	119.44	113.88	77.77	77.77	44.44
8:00	288.88	261.10	227.77	208.32	166.66
9 :00	480.54	427.76	377.76	358.32	297.21
10:00	633.31	558.31	458.32	455.54	419.43
11:00	755.53	666.6	530.54	541.65	522.20
12:00	799.97	711.09	580.53	583.31	563.87
13:00	805.53	716.64	608.31	594.42	583.31
14:00	755.53	647.20	561.09	530.54	522.20
15:00	597.20	538.87	474.98	491.65	413.87
16:00	441.65	372.21	386.10	363.87	333.32
17:00	261.10	238.88	233.32	191.66	197.21
18:00	105.55	99.99	111.10	69.44	55.55

fects of one key parameter on the overall system performance would normally require several cooling seasons and hence years to establish a conclusion. Also, it is extremely difficult to keep the performance of the system components to be constant over the entire experimental period as the components deteriorate with time. Therefore, it is extremely difficult and expensive to carry out experiments to investigate the influence of all the key parameters on the overall system performance of an existing solar-cooling system. The objective of this work is to model a complete solar absorption cooling system, comprising a solar collector, storage tank and an LiBr–water absorption chiller and to develop a simulation program for parametric study of this system. The developed program is used to simulate the cooling system with the help of meteorological data developed for Bahal. In the present work, modeling and simulation are done for proper sizing of flat-plate solar collectors with a water storage tank to match the load needed to the generator of the absorption system. The performance of a 10.5 kW solar-driven lithium bromide absorption cooling system is investigated numerically. In Section 2, the mathematical modeling of the solar absorption cooling system is provided, as also of absorption and solar collector systems. Section 3 presents the results and discussion pertaining to the validation of code. Section 4 concludes the work.

2. Mathematical model of solar absorption cooling system

Figure 1 shows the schematic diagram of the basic principle of solar absorption cooling system. This system has been the basis of most of the experience to date with solar airconditioning. Here, the solar energy is gained through the collector and is accumulated in the storage tank. Then, the hot water in the storage tank is supplied to the generator to boil off water vapor from a solution of lithium bromide + water. The water vapor is cooled down in the condenser and then passed on to the evaporator where it is again evaporated at low pressure, thereby providing cooling to the required space. Meanwhile, the strong solution leaving the generator to the absorber passes through a heat exchanger to preheat the weak solution entering the generator. In the absorber, the strong solution absorbs the water vapor

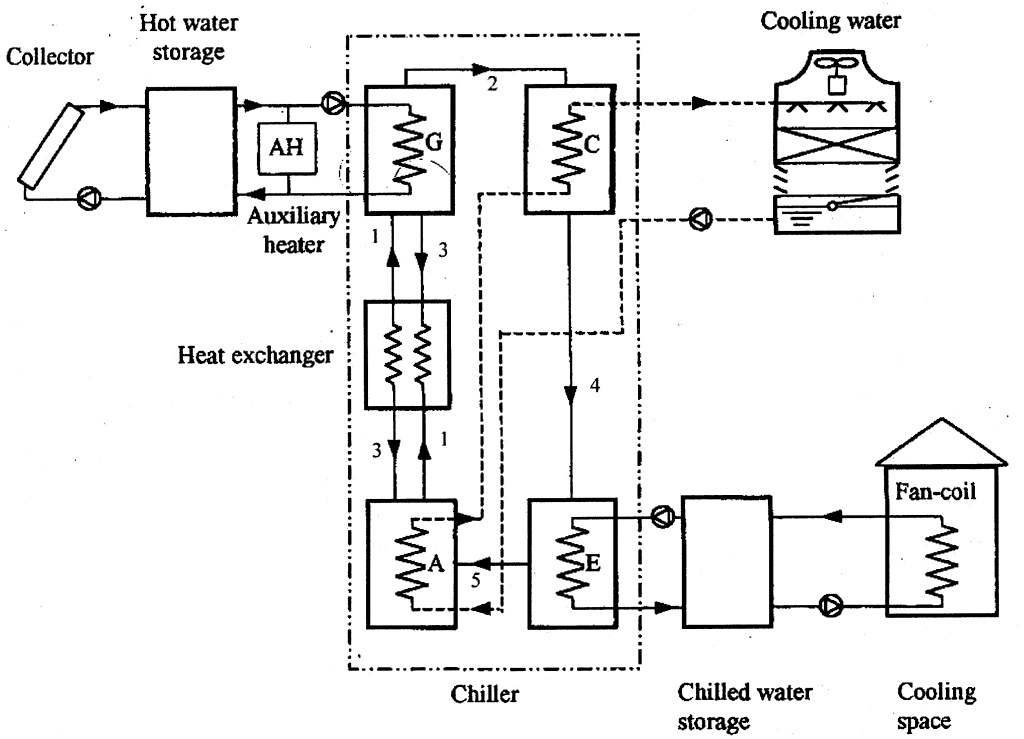

FIG. 1. Basic principle of solar absorption cooling system.

leaving the evaporator. Cooling water from the cooling tower removes the heat by mixing and condensation. Since the temperature of the absorber has a higher influence on the efficiency of the system than the condensing temperature, the heat rejection (cooling water) fluid is allowed to flow through the absorber first and then to the condenser. An auxiliary energy source is provided so that hot water is supplied to generator when solar energy is not sufficient to heat the water to the required temperature level needed by the generator. The mathematical modeling of complete solar-assisted absorption cooling system requires the modeling of absorption system as well as that of solar collector system separately.

2.1. *Modeling of the absorption cooling system*

To analyze the working conditions of the components of the system, i.e. the generator, absorber, evaporator, condenser and the heat exchanger, a control volume is taken across each component and standard mass and energy balances are performed and a computer program is developed for the cycle analysis. Necessary equations for modeling absorption cooling system are taken from Herold *et al.* [14].

Energy balance: Taking a control volume around each component, the rate of heat addition in the generator is the energy input to the cycle given by

$$Q_{\text{gen}} = h_2 m_2 + h_3 m_3 - h_1 m_1. \tag{1}$$

The rate of heat rejection out of the condenser is given by

$$Q_{\text{con}} = m_2(h_2 - h_4). \tag{2}$$

The rate of heat absorption in the evaporator is given by

$$Q_{\text{evap}} = m_4(h_5 - h_4). \tag{3}$$

The rate of heat rejection by the absorber is given by

$$Q_{\text{abs}} = h_5 m_5 + h_3 m_3 + h_1 m_1. \tag{4}$$

COP is defined according to Fig. 1 as follows:

$$\text{COP} = \frac{Q_{\text{evap}}}{Q_{\text{gen}}}. \tag{5}$$

The various enthalpies of the refrigerant and absorbent are calculated through simulating concentration charts using equations [15, 16]. The enthalpies of H_2O are expressed as a second-order polynomial in terms of respective temperatures at evaporator, condenser and generator as suggested by Stoeker [15]. The enthalpy h of the solution of H_2O–LiBr is expressed in a multivariable polynomial in terms of the solution temperature, T (°C), and solution concentration, X, through the absorber and generator unit as given in ASHRAE charts by:

$$h = \sum_0^4 A_n X^n + T \sum_0^4 B_n X^n + T^2 \sum_0^4 C_n X^n \tag{6}$$

where A, B and C are constant coefficients and are listed in ASHRAE [16].

2.2. *Solar energy modeling*

The solar collector field comprises several units of widely spread nonselective single glazing that collects and stores solar energy in a water storage tank. Each unit has an effective surface area of 2.44 m^2. The absorber plate is a black-painted steel plate with an emissivity of 0.11 and absorptivity of 0.92 and has 12 welded longitudinal copper tubes of 15 mm diameter. The collectors are set at an $f - 15°$ tilt angle facing south where f is the latitude of Bahal. The performance of the collector-tank system is simulated numerically using the theory of Hottel and Whiller, presented by Duffie and Beckman [17]. The useful solar energy collected is transferred to the hot liquid storage tank from which the generator of the absorption system is supplied with input thermal energy. Necessary equations for modeling solar energy are taken from Duffie and Beckman [17].

$$Q_u = A_c . I . h_c \tag{7}$$

where Q_u is the useful energy collected in system collectors, A_c, the collector area, I, solar insolation and h_c, the collector efficiency

$$h_c = F_R \cdot \left[(ta) - U_L \frac{T_{in} - T_o}{I} \right]. \tag{8}$$

In this equation, T_{in} is the collector inlet temperature and T_o, the environment temperature. A water storage tank is placed after the solar collector. Flat plate collector is considered in the simulation. Perfect mixing within the tank is assumed. If the rate of heat addition and removal for a reasonable time period of Δt are assumed to be constant, equations can be written for each time interval as suggested by Duffie and Beckman [17]:

$$T_{s,\text{new}} = T_{s,\text{old}} + \frac{\Delta t}{(m.C_{vw})_s}[Q_u - Q_L - (U.A)_S.(T_S - T_O)]. \tag{9}$$

In the above equations, Q_L is the extracted energy from the storage tank, T_s, the main storage temperature for the period and m, the storage tank mass. $(U.A)_s$ is taken as 11.1 W/K as suggested by Duffie and Beckman [17]. Here, the heat-transfer coefficient is assumed to be 0.72 W/m^{2}K for natural convection. An auxiliary heater at the exit of the storage tank boosts the temperature of the hot water from the storage tank temperature to the allowable reference temperature when the storage tank temperature drops below the allowable reference temperature. For this reason, the reference temperature can be considered to be exactly the minimum allowable hot water inlet temperature. The auxiliary heater capacity is calculated as follows:

$$Q_{\text{aux}} = m.C_{pw}.(T_{\text{ref}} - T_S), \tag{10}$$

where m is the mass flow rate used by the generator.

The fraction of the total load met by nonpurchased energy FNP is calculated as;

$$FNP = 1 - \frac{Q_{\text{aux}}}{Q_{\text{load}}} \tag{11}$$

where Q_{load} is exactly the same as Q_{gen} which is the generator load. Simulation includes inputs and outputs.

2.2.1. *Input data required*

The input data required for simulating the system consists of the following: system nominal capacity, generator temperature range, condenser temperature range, evaporator temperature range, absorber temperature, ambient temperature range, generator and condenser pressure, evaporator and absorber pressure, mass flow rate from generator to condenser, mass flow rate from absorber to generator, and mass flow rate from generator to absorber. The system has been designed for 10.5 kW constant cooling load. The output includes the surface area of the system components, COP and the fraction of the total met by FNP.

3. Results and discussion

3.1. *Validation*

The computer program developed has been validated by comparing some of the FNP results with a similar study like those by Ileri [18], by taking into consideration the effect of the reference temperature on the FNP. It can be seen from Table II that, as compared with Il-

Table II
Comparison of FNP for different reference temperatures of the present study with those of Ileri's [18] for the month of August

T_{ref} (°C)	FNP (%)	
	Present study	Ileri [18]
80	100	94
85	89	–
90	69	58
95	–	56

eri's study [18], the results of the present study for reference temperature effects show the same general behavior. Similar to our study, Ileri's study also shows that an 80°C reference temperature is the best solution. There is a good agreement between the two studies.

3.2. *Simulation results and discussion*

Simulation results are presented here for the performance of a 10.5 kW solar-driven lithium bromide absorption cooling system. Figure 2 depicts the effect of the hot water inlet temperatures on the system COP and the FR—an increase in this temperature results in the decrease of FR. This is due to increase in the mass fraction of concentration solution (X_G), while with an increase in this temperature, COP increases.

Figure 3 depicts the effect of hot water inlet temperature on the surface area of the system components. It can be seen that increase in this temperature results in the decrease of the absorber and solution heat exchanger surface area. As flow ratio decreases, the thermal energy extracted from the absorber also decreases and hence the temperature of the absorber increases, which further resulted in the increase of logarithmic mean temperature difference (ΔT_m) in the absorber and solution heat exchanger. By decreasing the heat capacity and increasing ΔT_m, heat transfer surface area normally decreases in these components.

Figure 4 depicts the effect of reference temperatures on FNP. The investigation is carried out between 353 and 368 K (approximately 80–95°C) because the increment in the system

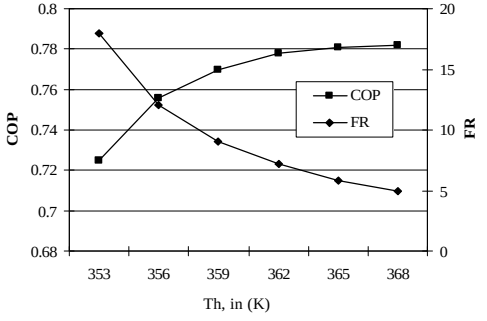

FIG. 2. The effect of hot water inlet temperatures on the system COP and FR (T_e = 280 K, Q_L = 10.5 kW, T_c = 306 K).

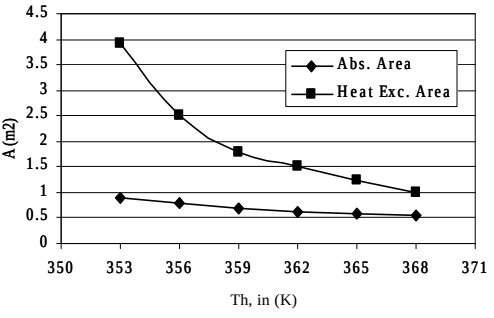

FIG. 3. The effect of hot water inlet temperatures on the surface area of the system components (T_e = 280 K, Q_L = 10.5 kW, $T_{cool,\ in}$ = 291 K).

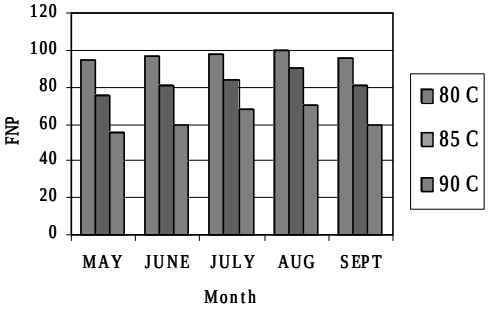

Fig. 4. The effect of reference temperatures on FNP.

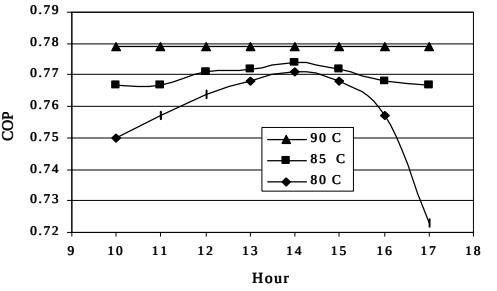

FIG. 5. The effect of reference temperatures on the system COP for a day in May.

COP slows down considerably after a certain temperature. Furthermore, boiling occurs above 95°C which is not desirable. To investigate the effect of storage tank reference temperature on the FNP, three reference temperatures, 80, 85 and 90°C, were taken into consideration. It can be seen from Fig. 4 that the 80°C reference temperature seems to be the best, as it gives better results than at higher reference temperatures. In this study, a reference temperature below 80°C was not investigated as it could cause a decrease in the system COP, and below it sufficient refrigerant vapor is not driven from the liquid solution.

Figure 5 depicts the effect of the reference temperatures on the system COP for a day in June. As shown, unlike the effects caused by reference temperature on FNP, increasing the reference temperatures boosts the system COP. Also, the COP remains unchanged at this high reference temperature (90°C).

Figure 6 depicts the effect of reference temperature on the storage tank temperature for a day in May. It can be seen that the storage tank temperature increases at high reference temperatures. This is due to decrease in generator load, which further resulted in the decrease of thermal energy extracted from storage tank at high reference temperatures.

Figure 7 depicts the effect of reference temperature on the auxiliary heater capacity for a day in May. It can be seen that greater usage of the auxiliary heater takes place at higher reference temperatures. This is due to the fact that in spite of the high storage tank temperature, the high reference temperature does not reach 90°C.

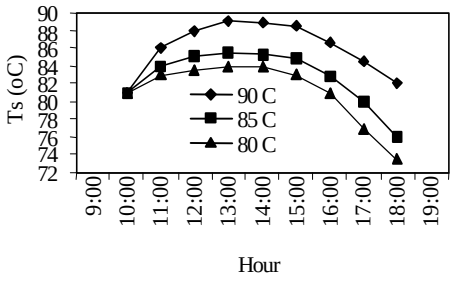

FIG. 6. The effect of reference temperatures on the storage tank temperatures for a day in May.

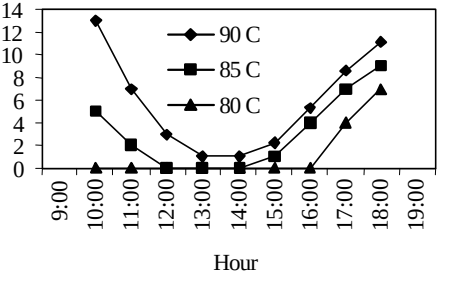

Fig. 7. The effect of reference temperatures on the auxiliary heater capacity for a day in May.

4. Conclusion

From the above study the following conclusions can be drawn:

1) The hot water inlet temperature is found to affect some of the surface area of the system components. Increasing this temperature decreases the absorber and solution heat exchanger surface area, while the dimensions of the other components remain approximately unchanged.

2) Although high reference temperature increases the system COP and decreases the surface area of the system components, lower reference temperature gives better results for FNP than high reference temperatures. For this study, an 80°C reference temperature is the best choice.

References

1. P. J. Wilbur, and C. E. Mitchell, Solar absorption air-conditioning alternatives, *Solar Energy*, **17**, 193–199 (1975).
2. V. Mittal, K. S. Kasana, and N. S. Thakur, Harnessing solar energy for absorption air-conditioning system**,** *Proc. Int. Congress on Renewable Energy Resources*, Allied Publishers, Pune, pp. 115–127 (2005).
3. M. A. Hammad, and M. S Audi, Performance of a solar LiBr–water absorption refrigeration system, *Renew. Energy* **2**, 275–282 (1992).
4. I. Haim, G. Grossman, and A. Shavit, Simulation and analysis of open cycle absorption systems for solar-cooling, *Solar Energy*, **49**, 515–534 (1992).
5. M. N. A. Hawlader, K. S. Novak, and B. D. Wood, Unglazed collector/regenerator performance for a solar-assisted open cycle absorption cooling system, *Solar Energy*, **50**, 59–73 (1993).
6. T. A. Ameel, K. G. Gee, and B. D. Wood, performance predictions of alternative, low cost absorbents for open cycle absorption solar cooling, *Solar Energy*, **54**, 65–73 (1995).
7. Z. F. Li, and K. Sumathy, Simulation of a solar absorption airconditioning system, *Energy Conversion Mgmt*, **42**, 313–327 (2001).
8. G. A. Florides , S. A. Kalogirou, S. A. Tassou, and L. C. Wrobel, Modelling and simulation of an absorption solar cooling system for Cyprus, *Solar Energy*, **72**, 43–51 (2002).
9. N. K. Ghaddar, M. Shihab, and F. Bdeir, Modeling and simulation of solar absorption system performance in Beirut, *Renewable Energy*, **10**, 539–558 (1997).
10. F. Assilzadeha, S. A. Kalogiroub, Y. Alia, and K. Sopiana, Simulation and optimization of a LiBr solar absorption cooling system with evacuated tube collectors, *Renewable Energy*, **30**, 1143–1159 (2005).
11. P. T. Tsilingiris, Theortical modelling of a solar airconditioning system for domestic applications, *Energy Conversion Mgmt*, **34**, 523–531 (1993).
12. Z. F. Li, and K. Sumathy, A computational study on the performance of a solar airconditioning system with a partitioned storage tank, *Energy*, **28**, 1683–1686 (2003).
13. Y. L. Liu, and R. Z. Wang, Performance prediction of a solar/gas driving double effect LiBr-H_2O absorption system, *Renewable Energy*, **29**, 1677–1695 (2004).
14. Krieth E. Herold, Reinhard Radermacher and Sanford A. Klein, *Absorption chiller and pump*, CRC Press (1994).
15. W. F. Stoeker, *Refrigeration and air conditioning*, International edn, McGraw-Hill (1987).
16. *ASHRAE Handbook of Fundamentals*, ASHRAE, Atlanta, USA (1985).
17. J. A. Duffie, and W. A. Beckman, *Solar engineering of thermal processes*, Wiley (1991).
18. A. Ileri, Yearly simulation of a solar-aided R22-DEGDME absorption heat pump system, *Solar Energy*, **55**, 255–265 (1995).

Nomenclature

A_c = collector area (m^2)
COP = coefficient of performance
FNP = the fraction of the total load met by nonpurchased energy (%)
FR = flow ratio ($X_A/(X_G - X_A)$)
h = enthalpy (KJ/Kg)
I = solar insolation (W/m^2)
k = heat conductivity (W/mK)
m = mass flow rate (kg/s)
Q = heat transfer rate (W)
Q_{aux} = auxiliary heater capacity (kW)
Q_L = extracted energy from the storage tank (kW)
Q_{load} = generator load (kW)
Q_u = useful energy (kW)
T = temperature (K, °C)
T_{in} = collector inlet temperature (°C)
T_o = the environment temperature (°C)
T_{ref} = reference temperature (°C)
T_s = storage tank temperature (°C)
U = overall heat transfer coefficient (W/m^2K)
X = weight fraction of LiBr
h_c = collector efficiency
Δt = time period (h)